Review Article

The physics of proton NMR

Robert L. Dixon and Kenneth E. Ekstrand

Department of Radiology, The Bowman Gray School of Medicine of Wake Forest University, Winston–Salem, North Carolina 27103

(Received 7 April 1982; accepted for publication 7 May 1982)

The physics of pulse NMR which is pertinent to an understanding of proton NMR imaging has been condensed and directed toward the medical physicist. The basic physical principles of spin manipulations using rf pulses are presented, and the relation between the quantum mechanical and the classical descriptions is covered in a rigorous fashion. The physics of relaxation is described and the relaxation times T_1 and T_2 are explained in some detail. Application of these spin manipulation techniques is illustrated by showing how they may be used in creating an image.

Key words: NMR, imaging

I. INTRODUCTION

Unlike the advent of computed tomography (CT), for which the fundamental physics of x-ray attenuation was well understood by the medical physics community, pulse nuclear magnetic resonance (NMR) techniques are relatively unfamiliar to most medical physicists and have a greater subtlety in terms of the numerous system properties which can be measured. In order for the physicist to understand the many different imaging methods used by the various NMR imaging groups, it is necessary to have a firm grounding in the basic principles of pulse NMR (which is quite different from continuous-wave NMR) and to understand the various spin manipulations which are possible.

Material from a wide variety of sources[1–6] has been condensed and directed toward the medical physicist who will be expected by the radiology community, in the immediate future, to understand and teach NMR. For simplicity proton NMR has been stressed. There have been some "popularizations" of NMR published in which quantum mechanics and physical rigor have been suppressed. This is not the case in the present work, since this approach leads to a superficial understanding.

A. Basic considerations

Before proceeding into the formalism, it is useful to consider a few simple analogies.

A proton by virtue of its spin angular momentum $\mathbf{S}$ possesses a proportional magnetic dipole moment $\boldsymbol{\mu} = \gamma \mathbf{S}$, where γ is the gyromagnetic ratio. If one thinks of a proton as a charged sphere, then a spinning proton represents a current flowing in a loop around the axis of rotation, thereby generating a dipolar magnetic field. We can therefore think of the proton as a "tiny magnet," having a magnetic moment $\boldsymbol{\mu}$.

The neutron also possesses a magnetic moment which is opposite to its spin direction. Although the neutron has no net charge, if the charge distribution were nonuniform (negative charge near the periphery and positive charge near the axis), then a spinning neutron would possess just such a magnetic moment. One should not carry this "spinning top" analogy too far, however, since the intrinsic spin angular momentum of the proton and neutron is no doubt due to some internal structure (quarks). Nuclei with either an odd number of protons or an odd number of neutrons also possess magnetic moments and are thus potential candidates for NMR, whereas even–even nuclei have zero magnetic moments. The unpaired nucleon is primarily responsible for the magnetic moment. If the unpaired nucleon is a proton, there can be an orbital as well as a spin contribution to the magnetic moment of the nucleus, although the shell model cannot accurately predict the magnitude of the nuclear moment.[23] Nuclei other than hydrogen which have been proposed as possible candidates for NMR imaging are ^{31}P,^{23}Na,^{19}F,^{13}C, etc., of which ^{31}P currently appears to be the most promising.[24] We will restrict our discussion to proton NMR since the sensitivity is several orders of magnitude greater than for other nuclei in tissue.

It is useful to first consider the behavior of a tiny magnet, such as a compass needle, in an external magnetic field (Fig. 1). The torque on the needle is given by $\boldsymbol{\mu} \times \mathbf{H}$ and the potential energy is $-\boldsymbol{\mu} \cdot \mathbf{H} = -\mu H \cos\theta$, where θ is the angle between $\boldsymbol{\mu}$ and $\mathbf{H}$. The potential energy is a minimum when $\boldsymbol{\mu}$ is aligned with the field ($\theta = 0$, $\cos\theta = 1$). A compass needle on a frictionless bearing would, however, never line up with the external field. If it were initially displaced by an angle θ_0, it would merely oscillate about the field direction with a constant amplitude θ_0. If a coupling between the magnet and its surroundings is added, such as bearing with friction (this is analogous to the spin–lattice interaction) and, if the nature of this coupling is such that the surroundings can absorb energy from the oscillating magnet, then the magnet will gradually relax until it is in its lowest energy state, i.e., aligned with the external field. In the case of a frictional damping force, the alignment would proceed exponentially with a time constant T_1 called the relaxation time.

The spins of the protons in a sample placed in a magnetic field will eventually arrange themselves such that the net magnetization (magnetic moment) of the sample $\mathbf{M}$ (where $\mathbf{M} = \Sigma \boldsymbol{\mu}_i$ is the vector sum of the individual proton magnet-

 0094-2405/82/060807-12$01.20

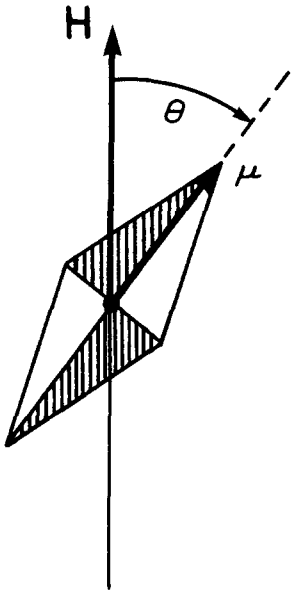

FIG. 1. Compass needle with magnetic moment μ in a magnetic field **H**.

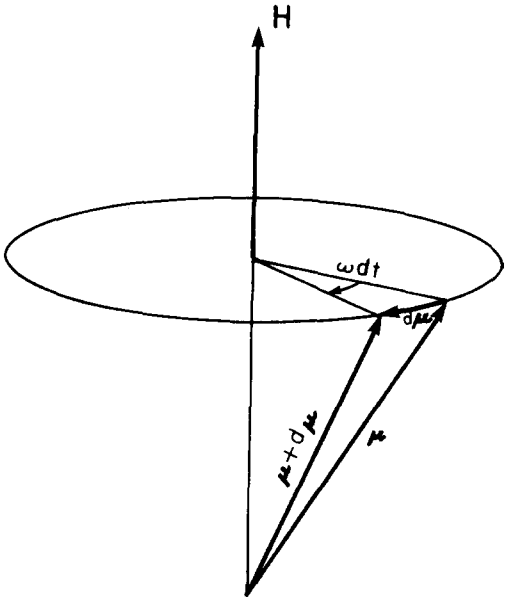

FIG. 2. Precession of a classical angular momentum **S**, having a proportional magnetic moment $\mu = \gamma S$, about a magnetic field **H**.

ic moments) lies along the field direction. This, however, requires coupling of the spins to an external system so that thermal equilibrium can be established.

II. CLASSICAL DESCRIPTION OF A SPIN IN A MAGNETIC FIELD

The classical motion of a magnetic moment μ associated with an angular momentum **S** is a bit different from that of a compass needle due to the angular momentum. The kinetic energy of such a system is contained primarily in its spinning motion. When a force is exerted on a spinning object, it tends to move at right angles to the force. A spinning gyroscope in a gravitational field does not fall over, but rather precesses around the gravitational field direction. The classical motion of a spin in a magnetic field can be derived by setting the torque equal to the rate of change of angular momentum.

$$\frac{d\mathbf{S}}{dt} = \boldsymbol{\mu} \times \mathbf{H}. \tag{1}$$

Since μ is proportional to **S**($\mu = \gamma$**S**), we have

$$\frac{d\boldsymbol{\mu}}{dt} = \boldsymbol{\mu} \times \gamma \mathbf{H}. \tag{2}$$

Since $d\mu$ is perpendicular to both μ and **H** (because of the cross product), the magnitude of μ remains constant, and the classical motion is a precession of μ about the magnetic field **H** (Fig. 2). It is easy to show from Eq. (2) and Fig. 2 that the angular frequency of precession is

$$\omega = \gamma H, \tag{3}$$

which is called the Larmor frequency.

There is still no tendency for a group of *isolated*, classical spins to align with the magnetic field—rather they would precess about it *ad infinitum*.

III. QUANTUM-MECHANICAL DESCRIPTION OF A SPIN IN A MAGNETIC FIELD

A quantum-mechanical treatment of a spin (i.e., a particle having a magnetic moment) in a magnetic field is easily made by setting the Hamiltonian equal to the potential energy $\mathscr{H} = -\boldsymbol{\mu}\cdot\mathbf{H}$. (Unlike a classical spinning top, the magnitude of the angular momentum of a quantum-mechanical spin cannot change, hence the "kinetic energy" associated with the spinning motion is constant and thus does not need to be considered in the Hamiltonian.) In a time-independent magnetic field $\mathbf{H}_0$ along the z axis, $\mathscr{H} = -\gamma H_0 S_z$, hence the stationary states of the system are the eigenstates of the angular momentum operator S_z and the energy levels are given by

$$E_{m_s} = -\gamma \hbar H_0 m_s, \quad -s \leqslant m_s \leqslant s. \tag{4}$$

For a particle with spin $\frac{1}{2}$ such as a proton, only two energy states are allowed, corresponding to spins parallel/antiparallel to the field ($m_s = \pm \frac{1}{2}$) as shown in Fig. 3, and having an energy separation of $\Delta E = \gamma \hbar H_0$. In the upper energy state, the spin direction is opposite the field direction ("spin down"). A transition from the lower to the upper state can be made by absorption of energy (for example, rf energy) of angular frequency ω_0, where $\hbar\omega_0 = \Delta E$; hence

$$\omega_0 = \gamma H_0. \tag{5}$$

ω_0 can be recognized as the classical Larmor precession frequency, $\omega_0 = \gamma H_0$. For a proton, this resonant frequency for

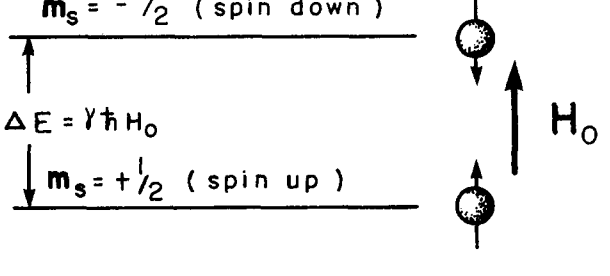

FIG. 3. Stationary energy states for a proton spin in a constant magnetic field $\mathbf{H}_0$.

energy absorption, $\nu_0 = \omega_0/2\pi$, is

$$\nu_0(\text{MHz}) = 4.258 H_0(\text{kG}). \tag{6}$$

Sometimes the magnetic field strength is expressed in Telsa (T) (0.1 T = 1 kG). rf irradiation of a spin system at this frequency, can cause spin–flip transitions. The transitions are magnetic dipole transitions which are influenced only by the magnetic component $\mathbf{H}'$ of the rf field, and then only by the x or y component of $\mathbf{H}'$ since the transition matrix element $\langle m_s'|\ \boldsymbol{\mu}\cdot\mathbf{H}'|m_s\rangle$ is nonzero only for μ_x and μ_y. rf irradiation at the resonant frequency can also cause de-excitation of a proton spin in the upper energy state by stimulated emission of a photon. Although the angular frequency ω_0 obtained from the Hamiltonian is the same as the classical Larmor frequency, the motion of a quantum-mechanical spin in one of the aforementioned stationary states should not be interpreted as a precession, since the wave function is independent of time, and the expectation value of the magnetic moment is time independent, i.e.,

$$\langle \mu_x \rangle = \langle \mu_y \rangle = 0,$$
$$\langle \mu_z \rangle = \pm \tfrac{1}{2}\gamma\hbar.$$

Recall that the expectation value represents the average result of a series of measurements on a group (or ensemble) of identical spins.

The preceding description of stationary states (time-independent wave functions in constant magnetic fields) is insufficient for understanding pulse NMR, since we need to follow the motion of the spins undergoing time-dependent perturbations by varying magnetic fields, where the wave functions are time dependent and consist of a mixture of the spin-up and spin-down states. For a proton spin having a wave function which is an equal mixture of both spin-up and spin-down states such that $S_x = \frac{1}{2}$ at $t = 0$, it can be shown[8] that $\langle \boldsymbol{\mu} \rangle$ evolves with time as

$$\langle \mu_x \rangle = \tfrac{1}{2}\gamma\hbar \cos\omega_0 t,$$
$$\langle \mu_y \rangle = -\tfrac{1}{2}\gamma\hbar \sin\omega_0 t, \tag{7}$$
$$\langle \mu_z \rangle = 0,$$

which describes a precession of $\langle \boldsymbol{\mu} \rangle$ in the xy plane.

We are fortunate in this regard to be able to make the following simplification. We cannot observe the behavior of a single spin, but rather we observe the collective motion of a group of spins (an ensemble) via the net magnetization $\mathbf{M}$. The expectation value of the magnetic moment of an ensemble of spins (i.e., the average magnetic moment for the ensemble) follows the quantum-mechanical rule for the equation of motion of an operator[7]

$$\frac{d}{dt}\langle \boldsymbol{\mu} \rangle = \frac{i}{\hbar}\langle [\mathscr{H}, \boldsymbol{\mu}] \rangle, \tag{8}$$

where $[\mathscr{H}, \boldsymbol{\mu}]$ is the commutator of the Hamiltonian $\mathscr{H}$ and $\boldsymbol{\mu}$. It may be shown in a straightforward manner,[9] using the commutation properties of angular momentum operators, that

$$\frac{d}{dt}\langle \boldsymbol{\mu} \rangle = \langle \boldsymbol{\mu} \rangle \times \gamma\mathbf{H}. \tag{9}$$

This is a general result that is valid for a time-dependent magnetic field $\mathbf{H}$, and is the same as the equation of motion for a classical spin with an associated magnetic moment.

For an ensemble of N noninteracting spins, the net magnetization, which is the observable quantity, is given by

$$\mathbf{M} = \mathrm{N}\langle \boldsymbol{\mu} \rangle, \tag{10}$$

hence $\mathbf{M}$ satisfies the classical equation of motion

$$\frac{d\mathbf{M}}{dt} = \mathbf{M} \times \gamma\mathbf{H}. \tag{11}$$

Thus, even though individual spins may undergo complicated behavior, the net magnetization $\mathbf{M}$, which is the observable quantity, follows the familiar classical equation, i.e., in a constant magnetic field, $\mathbf{M}$ will precess around the field at the Larmor frequency.

IV. MOTION OF M IN AN RF FIELD

We have shown for a system of noninteracting spins that the magnetization $\mathbf{M}$ follows Eq. (11).

For a static magnetic field $\mathbf{H}_0$ along the z axis, $\mathbf{M}$ will precess around the field (in a clockwise direction when viewed along the z axis) at the Larmor frequency $\omega_0 = \gamma H_0$.

If an rf coil is wound around the sample along the x axis and driven with an rf oscillator at frequency ω, an oscillating magnetic field $\mathbf{H}_x(t)$ is generated along the x axis which can be written as

$$\mathbf{H}_x(t) = \mathbf{i}2H_1 \cos\omega t. \tag{12}$$

Since the magnitude of this oscillating field is small compared to the static field $\mathbf{H}_0$, it might be expected to have little effect on the motion of $\mathbf{M}$. (For pulse NMR $H_x \sim 100$ G, whereas $H_0 \sim 10^3$ G.)

It is useful to decompose $\mathbf{H}_x(t)$ into two rotating components $\mathbf{H}_x = \mathbf{H}_1 + \mathbf{H}_1'$, where

$$\mathbf{H}_1' = H_1[\mathbf{i}\cos\omega t + \mathbf{j}\sin\omega t\,],$$
$$\mathbf{H}_1 = H_1[\mathbf{i}\cos\omega t - \mathbf{j}\sin\omega t\,], \tag{13}$$

so that $\mathbf{H}_1$ rotates clockwise in the xy plane viewed from above (the same direction as $\mathbf{M}$) as shown in Fig. 4, and $\mathbf{H}_1'$ rotates counterclockwise. (It is easy to verify this rotation by evaluating $\mathbf{H}_1$ at ωt values of 0°, 90°, 180°, and 270°.) Since the torque exerted on $\mathbf{M}$ by the rf field is $\mathbf{M}\times\gamma\mathbf{H}_x$, and since $H_1 \ll H_0$, it can be seen that this torque is small compared to the precessional driving torque due to $\mathbf{H}_0$, $\mathbf{M}\times\gamma\mathbf{H}_0$, and it can therefore have no great effect unless it remains constant for a long period of time. Since $\mathbf{H}_1'$ rotates in the opposite sense to $\mathbf{M}$, it is clear that the torque exerted will average to zero, hence we can ignore $\mathbf{H}_1'$ and write Eq. (11) as

$$\frac{d\mathbf{M}}{dt} = \mathbf{M}\times\gamma[\mathbf{H}_0 + \mathbf{H}_1(t)]. \tag{14}$$

It is also clear that $\mathbf{H}_1$ can have no great effect unless it rotates at the same angular frequency at which $\mathbf{M}$ precesses, so that it remains in constant phase with $\mathbf{M}$. That is, there is no significant effect unless the rf frequency ω is equal to the Larmor precession frequency $\omega_0 = \gamma H_0$. If $\omega \neq \omega_0$, $\mathbf{H}_1$ would either outrun or fall behind $\mathbf{M}$ and the effect would average to zero, i.e., $\mathbf{H}_1$ would only cause $\mathbf{M}$ to wobble a bit. If, however, $\omega = \omega_0$, then $\mathbf{H}_1$ stays in a constant position relative to $\mathbf{M}$. Thus, even though $\mathbf{H}_1$ exerts a small torque on $\mathbf{M}$,

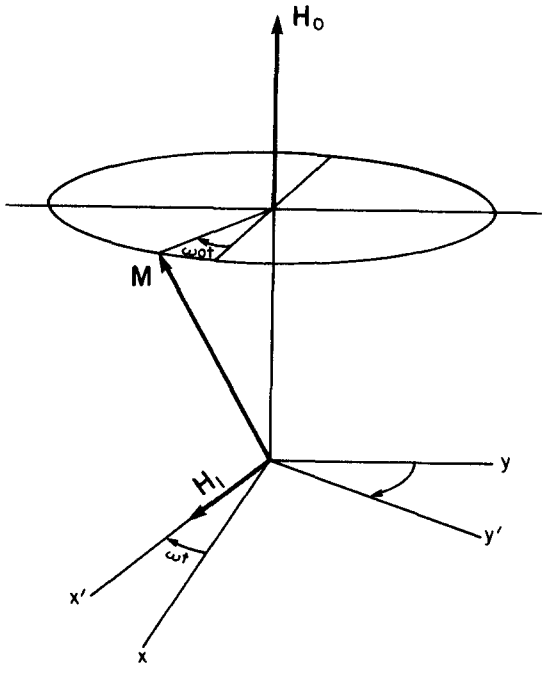

FIG. 4. Rotating frame axes x',y' rotate about the z axis with the frequency ω of the applied rf field $\mathbf{H}_1$. $\mathbf{H}_1$ is fixed in the rotating frame along the x' axis. The magnetization $\mathbf{M}$ precesses about the field $\mathbf{H}_0$ in the same sense as $\mathbf{H}_1$ but with frequency ω_0.

the torque is constant; and, if the torque lasts over many precessions of $\mathbf{M}$, it can have a significant effect. That is, if the rf signal is applied at the resonant frequency ω_0 for a time large compared to the Larmor precessional period $2\pi/\omega_0$, it will cause a significant effect on $\mathbf{M}$. This description is the classical explanation of magnetic resonance.

Equation (14) can be solved by looking at the motion in a frame of reference rotating with the applied rf field $\mathbf{H}_1$ at angular frequency ω as shown in Fig. 4. The rotating frame axes are denoted by (x',y',z'), however, the z' axis is coincident with the z axis of the laboratory system (x,y,z). One can think of the x' and y' axes as being fixed to a turntable rotating with angular frequency ω about the vertical (z',z) axis, whereas the xyz axes are stationary in the laboratory. The field $\mathbf{H}_1$ lies along the x' axis and rotates with it (Fig. 4).

It can be shown[10] that the time derivative of a vector in the laboratory system $d\mathbf{M}/dt$ can be related to its time derivative in a coordinate system rotating about the z axis with an angular velocity $\Omega = -\omega\mathbf{k}$ as

$$\frac{d\mathbf{M}}{dt} = \frac{\delta\mathbf{M}}{\delta t} + \Omega \times \mathbf{M}, \tag{15}$$

where $\delta\mathbf{M}/\delta t$ is the derivative in the rotating system. That is, a vector $\mathbf{M}$ fixed in the rotating system ($\delta\mathbf{M}/\delta t = 0$) would exhibit a time derivative in the lab system of $\Omega \times \mathbf{M}$, which we recognize as a precession about the z axis. Applying this transformation to Eq. (14), the motion of $\mathbf{M}$ in the rotating system can be determined as

$$\frac{\delta\mathbf{M}}{\delta t} = \mathbf{M} \times \gamma\mathbf{H}_{\text{eff}}, \tag{16}$$

where

$$\mathbf{H}_{\text{eff}} = (H_0 - \omega/\gamma)\mathbf{k} + H_1\mathbf{i}'. \tag{17}$$

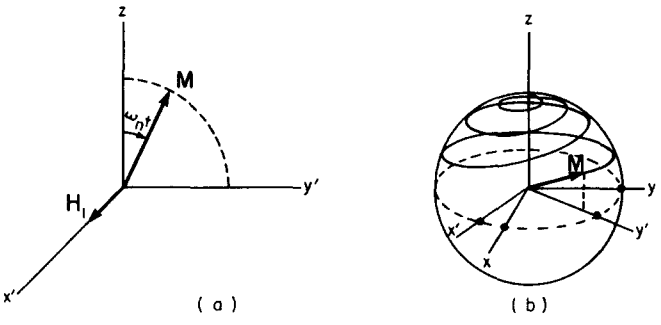

FIG. 5. Nutation of $\mathbf{M}$ away from its equilibrium position along the z axis under the influence of rf irradiation $\mathbf{H}_1$ at the resonant frequency ω_0 as seen in (a) the rotating frame and (b) the laboratory frame.

Thus the motion of $\mathbf{M}$ in the rotating frame is the same as the familiar equation of motion [e.g., Eq. (11)] with the field replaced by an effective field $\mathbf{H}_{\text{eff}}$. Note that $\mathbf{H}_{\text{eff}}$ is independent of time, i.e., it is fixed in the rotating frame. The motion in the rotating frame is therefore simply a precession of $\mathbf{M}$ about $\mathbf{H}_{\text{eff}}$. At resonance ($\omega = \gamma H_0$) note that $\mathbf{H}_{\text{eff}} = H_1\mathbf{i}'$ lies entirely in the xy plane along the rotating x' axis. Thus if $\mathbf{M}$ initially lay along the z axis, the motion in the rotating frame would be a nutation of $\mathbf{M}$ about the x' axis with frequency $\omega_n = \gamma H_1$ as shown in Fig. 5(a). The vector $\mathbf{M}$ remains in the $y'z$ plane, rotating about the x' axis at a frequency ω_n, where $\omega_n \ll \omega_0$, for as long as the rf irradiation persists. Figure 5(b) shows the corresponding motion in the laboratory frame. In the lab system, $\mathbf{M}$ simply spirals down from the z axis over many precessional periods since $\omega_n \ll \omega_0$.

If ω is not near resonance, $\mathbf{H}_{\text{eff}}$ lies just a bit off the z axis in the $x'z$ plane. Since $\mathbf{M}$ must precess about $\mathbf{H}_{\text{eff}}$, $\mathbf{M}$ would merely nutate a little. That is, if $\mathbf{M}$ initially lay along the z axis, it would periodically dip away from the z axis by a small angle and return to the z axis again, with $\mathbf{H}_{\text{eff}}$ defining the center of the cone of nutation.

To observe this resonance phenomenon, an rf pulse at frequency ω_0 of duration Δt can be applied such that

$$\omega_n \Delta t = \gamma H_1 \Delta t = \pi/2.$$

(This is called a 90° pulse since such a pulse will rotate the magnetization by 90°.) If $\mathbf{M}$ initially lies along the z axis, as it will at equilibrium, it will be rotated by 90° such that, at the end of the pulse, it will lie along the y' axis in the rotating frame [Fig. 6(a)], which means that it will precess in the xy plane in the lab system as shown in Fig. 6(b). $\mathbf{M}$ will continue to precess in the xy plane at frequency ω_0, as shown, after termination of the rf pulse. This motion can be observed as follows. Such a motion is analogous to spinning a magnet having a dipole moment $\mathbf{M}$ around inside the rf coil (which you recall is wrapped around the lab x axis). Such a changing magnetic flux will induce an alternating emf in the coil at frequency ω_0 which may be detected by connecting the coil to a receiver after termination of the rf pulse from the transmitter. This signal is the so-called free-precession (or free-induction) signal. The magnetic induction $\mathbf{B}$ produced in a magnetized sample having magnetization $\mathbf{M}$ is $\mathbf{B} = 4\pi\mathbf{M}$.[11] The magnetic flux through a coil having n turns and a cross-sectional area A is approximately

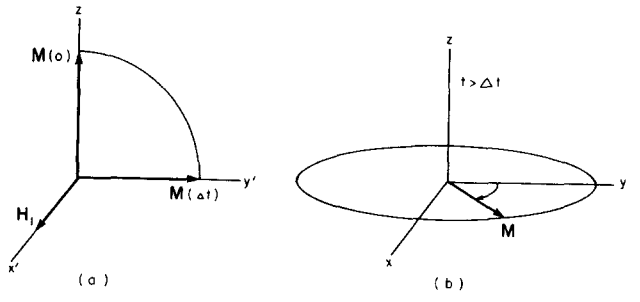

FIG. 6. (a) Nutation of **M** away from its equilibrium position onto the rotating frame y' axis produced by a 90° rf pulse at resonance. (b) Continued free precession of the magnetization **M** in the laboratory equatorial plane after termination of the rf pulse.

$$\Phi = B_x nA = 4\pi M_x nA.$$

If a 90° pulse is applied to a sample initially at equilibrium having a magnetization M_0, then, following the pulse, M_x will have the form $M_x = M_0 \sin \omega_0 t$. The emf induced in the coil is therefore

$$V = -\frac{1}{c}\frac{d\Phi}{dt} = (4\pi/c)nA\, M_0\omega_0 \cos \omega_0 t. \tag{18}$$

The maximum signal strength will be produced by a 90° rf pulse, since it is only the component of **M** in the transverse xy plane which induces any signal in the coil. A pulse of duration longer or shorter than $\Delta t = \pi/2\gamma H_1$ will produce a smaller signal, and a 180° pulse ($\Delta t = \pi/\gamma H_1$) will produce no signal at all since **M** will be rotated over to the minus z axis, thereby having no transverse component. The length of these rf pulses are generally of the order of microseconds and are much shorter than the relaxation times encountered in liquids or tissues. For $H_1 = 50$ G, a 90° pulse would have a length of about 1.2 μs.

Recall it has been assumed that the system of protons we have been considering neither interact with each other nor their surroundings, save for the externally applied magnetic field $\mathbf{H}_0$, which has been presumed to be uniform over the sample (i.e., the same for all protons). In this case, following say a 90° pulse, the protons will freely precess in the xy plane, "singing" together in unison into the pickup coil. They would sing forever under the aforementioned idealized conditions, however, relaxation will eventually take place as we will discuss in the next section.

It is worthy of note at this point that the applied oscillating field $H_x = 2H_1 \cos \omega t$ resulted in $\mathbf{H}_1$ lying along the x' axis in the rotating frame. It can be shown that if the rf signal is phase shifted by 90° such that $H_x = 2H_1 \sin \omega t$, then an $\mathbf{H}_1$ is generated along the y' axis in the rotating frame. Thus $\mathbf{H}_1$ can be put along any axis in the rotating frame simply by electrically phase shifting the rf signal (without moving the coil).

The strength of the free-precession signal at resonance will increase as the square of the external magnetic field strength since (i) the initial (equilibrium) magnetization is larger in a larger field, and (ii) the emf induced by the rotating magnetization depends on its time derivative and hence is proportional to the precession frequency. Since the thermal equilibrium population ratio of the spin-up and spin-down states depicted in Fig. 3 is given by $\exp(-\Delta E/kT)$, it can be shown that the equilibrium magnetization M_0 for N proton spins having $\mu = \frac{1}{2}\hbar\gamma$, is given by

$$M_0 \simeq \left(\frac{N\mu^2}{kT}\right) H_0. \tag{19}$$

This relation will be derived in Sec. V.

Using Eq. (18) for the induced emf, replacing ω_0 by γH_0 and M_0 with Eq. (19) the free-precession signal following a 90° pulse is

$$V = (4\pi/c)nA\gamma H_0^2 \left(\frac{N\mu^2}{kT}\right) \sin \omega_0 t. \tag{20}$$

Since the strength of the free-induction signal is proportional to the square of the static magnetic field, the importance of a strong magnetic field in improving the signal-to-noise ratio is evident. It is for this reason that NMR spectroscopy is generally done at frequencies of 24 MHz and above. The signal-to-noise ratio is, however, more complex than the above expression for the induced emf. The noise generated in the coil depends on the coil resistance which in turn depends on frequency, due to the fact that at the frequencies of interest in NMR the current in the coil flows near the surface of the wires, and the skin depth is frequency dependent. For spectroscopy (small samples), the frequency dependence of the signal-to-noise ratio[22] is approximately $\omega_0^{7/4}$. For NMR imaging, noise is also generated by the patient (e.g., induced magnetic eddy currents) as described by Hoult.[20] In addition, at very high frequencies, the rf may be significantly attenuated by the patient.

We can at this point pause to get a brief glimpse of the powerful imaging capabilities available with NMR. If a 90° pulse is applied to an entire sample (e.g., a human head) in a uniform field $\mathbf{H}_0$, the spins will all precess in the xy plane at the resonant frequency $\omega_0 = \gamma H_0$. If, after termination of the 90° rf pulse, it could be arranged (by applying magnetic field gradients) to have the z component of the magnetic field slightly different (and unique) at each spatial point $\mathbf{r}$ in the sample in a known fashion, then the precession frequency will be a function of position $\omega_0(\mathbf{r})$. After application of such gradients, protons at each spatial point will begin to "sing" (precess) at different frequencies. By listening to one frequency at a time one could tell, by the signal strength, the proton density at each spatial point. Or, more efficiently yet, one could perform a spectral analysis of the pickup coil signal $I(t)$ and derive the spatial information using a Fourier transformation.

$$F(\omega) = \int_{-\infty}^{\infty} I(t) e^{-i\omega t} dt. \tag{21}$$

The magnitude of $F(\omega)$ at each ω, gives the relative proton density at the corresponding spatial point $\mathbf{r}$ if $\omega(\mathbf{r})$ is known. Thus, in principle, with a single rf pulse one could obtain three-dimensional information from which to construct an image without resorting to any CT reconstruction techniques whatsoever. (In reality, it is not quite this simple.)

V. RELAXATION

A. T_1 relaxation

In order to understand relaxation, it is necessary to look again at the quantum-mechanical model for the energy states of a proton in a magnetic field (Fig. 3).

From atomic physics, we recall that an atom in an excited state will deexcite in $\sim 10^{-8}$ s by spontaneous emission. In addition, electromagnetic radiation having a frequency such that $h\nu$ is equal to the spacing between energy levels can cause either excitation of the atom if it is in the lower energy state; or, with equal probability, the deexcitation of an atom in the upper state by stimulated emission of a photon. Theoretically, the situation is the same in NMR except that a proton in the upper energy state (spin opposite the applied field) has a characteristic time for spontaneous emission of $\sim 10^{19}$ yr due to the fact that the spontaneous emission probability is proportional to the cube of the frequency.[12] A 90° rf pulse causes equal population of the two spin states ($M_z = 0$); however, after termination of the rf pulse, we know from experience that the net magnetization will return to the z axis in a time of the order of 1 s, which means that at equilibrium there are more protons in the lower (spin-up) energy state than in the upper (spin-down) state. The reason for the excess population in the lower state is because our system of proton spins, through interaction with the surroundings (the lattice), has come into thermal equilibrium with the surroundings. If the number of protons in the spin-up and spin-down states is denoted by n_+ and n_-, respectively, then at equilibrium the relative populations are given by the Boltzman distribution

$$\frac{n_-}{n_+} = e^{-\Delta E/kT}, \tag{22}$$

where ΔE is the spacing of the energy levels ($\Delta E = \hbar\omega_0$) and T is the temperature. The net z component of the magnetization is proportional to the excess population in the spin-up state

$$M_z = (n_+ - n_-)\mu, \tag{23}$$

where $\mu = \frac{1}{2}\hbar\gamma$ is the proton magnetic moment ($\langle \mu_z \rangle = \pm \frac{1}{2}\hbar\gamma$). Since $\Delta E \ll kT$ for NMR, the excess population is very small. For a total of $N = (n_+ + n_-)$ proton spins, it is easy to show, using Eqs. (22) and (23) that the equilibrium value of $\mathbf{M}$ is

$$M_0 = N\mu \tanh\left(\frac{\Delta E}{2kT}\right). \tag{24}$$

Since $\Delta E \ll kT$ and $\Delta E = \gamma\hbar H_0 = 2\mu H_0$, Eq. (24) may be approximated by

$$M_0 \approx \left(\frac{N\mu^2}{kT}\right) H_0, \tag{25}$$

hence it can be seen that M_0 is proportional to the external field strength H_0 and the square of the magnetic moment μ.

The characteristic time for return to thermal equilibrium is called the spin–lattice relaxation time T_1, such that the z component of the magnetization obeys

$$\frac{dM_z}{dt} = -\frac{(M_z - M_0)}{T_1}, \tag{26}$$

which is called the Bloch equation.[21] This form of the more general Bloch equations[21] applies only in the absence of externally applied rf fields; however, it is all we shall require, since the duration of the rf pulses used is short compared to the relaxation times encountered in tissues. That is, we can assume Eq. (16) describes the motion of $\mathbf{M}$ during the rf pulse, and Eq. (26) applies after (or between) rf pulses. Solving Eq. (26) following a 90° pulse with the initial condition $M_z(0) = 0$, we have

$$M_z(t) = M_0(1 - e^{-t/T_1}), \tag{27}$$

hence Eq. (26) predicts an exponential return to equilibrium with time constant T_1.

In order for a spin system initially perturbed from equilibrium by an rf pulse to return to equilibrium (say a 180° pulse which gives an excess population in the upper state), energy must be transferred to the surroundings (the lattice). This is evident from the fact that the total energy of the spin system in a field $\mathbf{H}_0$ is given by

$$E = -\mathbf{M}\cdot\mathbf{H}_0 = -M_z H_0,$$

hence any change in the net z component of the magnetization after termination of an rf pulse requires an energy transfer to or from the lattice. The transitions from the upper to the lower energy states are not spontaneous but are stimulated by fluctuating magnetic fields produced by molecular motions. If these internal fluctuating fields have frequency components at the resonant (Larmor) frequency, they can stimulate the deexcitation of protons in the upper state, this energy being transferred from the spin system into thermal kinetic energy of the lattice (or heat reservoir). T_1 is therefore a measure of the time required to establish thermal equilibrium between the spins and their surroundings. If a static field $\mathbf{H}_0$ is applied to an initially unmagnetized sample, T_1 is also the characteristic time for the equilibrium magnetization $\mathbf{M}_0$ to be established.

These fluctuating internal fields can be produced by a wide variety of sources. One source is the dipole–dipole interaction between nuclear spins. That is, a spin by virtue of its magnetic moment $\boldsymbol{\mu}$ can exert a magnetic field on a neighboring spin of the order μ/r^3, where r is the separation distance.[13] The separation distance of the two protons in a water molecule is 1.5 Å, hence the magnitude of this local field is about 4 G. Let us take the point of view of a proton on a water molecule, and suppose that both protons in the H_2O molecule are in a spin-up state. They will both remain aligned with the external field $\mathbf{H}_0$ as the molecule tumbles in its random thermal motion, and hence one proton feels a fluctuating magnetic field due to the magnetic moment of its neighbor changing its relative position. In addition, other molecules which collide with the H_2O molecule will present it with a variety of neighboring spins in random orientations which will also produce a fluctuating magnetic field at the position of the proton.

Paramagnetic ions can provide a powerful relaxation mechanism. These ions have an unpaired electron and hence have a magnetic moment equal to that of an electron spin. The magnetic moment of an electron spin is 700 times that of a proton, hence a very large fluctuating field can be provided by the random thermal motion of paramagnetic ions. Exam-

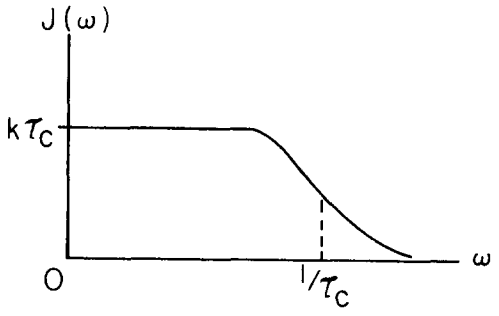

FIG. 7. Spectral power density $J(\omega)$ of random molecular motion for a correlation time τ_c.

ples of paramagnetic ions are transition group elements (Fe,Mn,Cu,Cr,Co,Ni,Ti) and rare-earth elements. Adding only 20 ppm of Fe^{3+} to pure water will reduce T_1 from 3.6 s to 20 ms. The O_2 molecule is also paramagnetic, hence dissolved oxygen can also shorten the T_1 of water. Paramagnetic ions can therefore serve as contrast media for NMR imaging.

It is only the component of these fluctuating magnetic fields at the Larmor frequency which is efficient in inducing T_1 relaxation. Although the time behavior of the thermal motion is random, it can be Fourier analyzed to determine its component at the Larmor frequency. The method of analysis of this random motion is the following. The molecular environment is considered to be constant for a time, and then changes abruptly but randomly to another configuration. The probability of the environment not changing in a time t is proportional to $\exp(-t/\tau_c)$, where τ_c is the correlation time, or a measure of the average time required for the environment to change significantly. For water at room temperature, $\tau_c \sim 10^{-12}$ s. The magnitude of τ_c depends on the temperature, i.e., at high temperatures where molecular motion is rapid, τ_c will be short. A Fourier analysis of this type of function gives a spectral power density

$$J(\omega) = k\frac{\tau_c}{1+\omega^2\tau_c^2}, \tag{28}$$

where k is a function of the spin separation distance. The form of $J(\omega)$ is shown in Fig. 7.

It is the magnitude of $J(\omega)$ at the Larmor frequency ω_0 which is important in stimulating relaxation. If τ_c is very long such that $\omega_0 \gg 1/\tau_c$, there are no components of molecular motion at the Larmor frequency, hence relaxation times would be very long. If τ_c is very short, such that $\omega_0 \ll 1/\tau_c$, we have a wide frequency range of molecular motion, however, the magnitude of $J(\omega)$ at any frequency is reduced since the total power available for molecular motion is constant and it is spread over a wide frequency range. From Fig. 7, we see that the intercept of $J(\omega)$ at zero frequency is proportional to τ_c such that $\int_0^\infty J(\omega)d\omega = \text{constant}$. Relaxation is most efficient (T_1 is shortest) when $\omega_0 \sim 1/\tau_c$.

It can be seen from the above that relaxation times will depend on both resonant frequency and temperature.

B. T_2 relaxation

T_1 (spin–lattice) relaxation is concerned with the z component of the magnetization. There is, however, another characteristic relaxation time called T_2 (or spin–spin) relaxation which is a measure of the time of disappearance of the transverse component of the magnetization. When we tip the magnetization into the transverse plane with a 90° pulse, we have a coherent mixture of spin states such that the precessing spins maintain a constant phase relationship to each other during precession. Processes which affect this phase coherence cause the disappearance of M_x and M_y and hence loss of the free-induction signal. Of course, T_1 relaxation processes can cause loss of phase coherence since random spin–flip transitions are occurring, and in many cases T_2 is equal to T_1; however, loss of phase coherence may also be produced by interactions which do not transfer energy from the spin system to the lattice (e.g., two interacting spins could mutually flip each other, resulting in no net change in the z component). Thus, in general, $T_2 \leqslant T_1$.

T_2 relaxation can be understood as follows. If the magnetization is tipped into the xy plane with a 90° pulse, the individual protons would remain in phase with each other if each one felt exactly the same magnetic field $\mathbf{H}_0$. If, however, different protons in the system were to feel slightly different magnetic fields, they would undergo free precession at slightly different frequencies. This would cause the transverse component of the magnetization $\mathbf{M}$ to disappear as the protons got out of phase with each other, and the free-induction signal would therefore disappear. The free-induction signal is often called the FID (free-induction decay).

1. Static field inhomogeneity

Let us assume a field inhomogeneity (which is constant in time) such that various groups of protons in the sample experience slightly different fields. If $\mathbf{m}_i$ denotes the magnetization due to the ith proton group, then the net magnetization (which is the observable quantity) is given by the vector sum

$$\mathbf{M} = \sum_i \mathbf{m}_i. \tag{29}$$

Following a 90° pulse, all the $\mathbf{m}_i$ will lie along the y' axis in the rotating frame, however, due to the slightly different free-precession frequencies, they will dephase in the rotating frame as depicted in Fig. 8 and the vector sum $\mathbf{M}$ will gradually disappear.

That is, if the field over the sample varies over the range $H_0 \pm \Delta H$, the set of spins which feel the field H_0 will remain fixed in the rotating frame (which rotates in the lab with a frequency $\omega_0 = \gamma H_0$); however, those spins that feel a field $H_0 + \Delta H$ will precess faster, and those experiencing a field

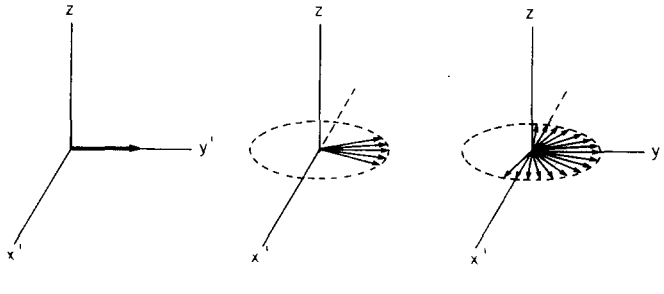

FIG. 8. Dephasing of spins in the rotating frame due to differences in the local magnetic field felt by the various spins.

$H_0 - \Delta H$ will precess slower. The net magnetization M will completely disappear when the fastest and slowest group of spins dephase in the rotating frame by 180°. This will occur in a time $\pi/\gamma\Delta H$. The time required for the free-induction signal to decay by $1/e$, assuming an exponential decay, is $\sim 1/\gamma\Delta H$. A 90° pulse has been chosen merely for ease of illustration. The transverse component of the magnetization would disappear in the same amount of time following an rf pulse of less than 90° or greater than 90°.

This type of field inhomogeneity could result from either a nonuniform external field or from an internal field due to neighboring spins. That is, a spin, by virtue of its magnetic moment μ, can exert a magnetic field on a neighboring spin of the order of μ/r^3, where r is the separation distance. The magnitude of the field generated by a proton at a distance of 2 Å is 1.8 G. This would result in a dephasing time $1/\gamma\Delta H$ of only 20 μs. In a solid, where neighboring spins maintain a fixed relationship to each other, transverse relaxation times are relatively short. Decay of the transverse magnetization caused by internal fields (static or otherwise) is regarded as true T_2 relaxation, whereas decay produced by external field inhomogeneity is not a T_2 process.

2. T_2 relaxations due to fluctuating internal fields

In a liquid, the protons in our system are the nuclei of hydrogen atoms on molecules which are tumbling and translating about with thermal kinetic energies, such that the internal magnetic field does not contain a large static component. This will increase T_2 significantly over that of a solid, e.g., T_2 of water is ~ 3 s whereas T_2 for ice is $\sim 10\,\mu$s. Even if the time average of this randomly fluctuating field were zero, it could still cause transverse (T_2) relaxation—particularly if the fluctuating field has frequency components at the Larmor frequency. Recall that a small oscillating $\mathbf{H}_1$ field could produce a significant effect if its frequency were near the resonant frequency, since at that frequency it would remain fixed in the rotating frame of the magnetization and could exert a constant torque over a period of time. The same holds true for a fluctuating internal field. It can cause transverse dephasing by causing the proton spins to execute a random walk in the rotating system away from the y' axis (Fig. 8).

Decay of the transverse magnetization due to these *internal* fields (static or fluctuating) proceeds exponentially with a time constant denoted by T_2. Since it is the transverse magnetization component in the rotating frame which produces the signal, the free-induction signal would decay with a time constant T_2 (if the external field were perfectly homogeneous). T_2 is called the spin–spin relaxation time. For pure wate, T_2 is approximately 3 s.

In a liquid, the major factor influencing the decay of the transverse magnetization and the FID is the inhomogeneity of the external field. For example, if we have an external magnetic field of 1000 G which is uniform over the sample to $\pm$ 10 ppm ($\Delta H/H_0 = 10^{-5}$), the transverse decay time would be $1/\gamma\Delta H = 3.7$ ms. The FID signal will decay with an effective time constant T_2^*, where

$$\frac{1}{T_2^*} = \gamma\Delta H + \frac{1}{T_2}. \tag{30}$$

If the true intermolecular relaxation time T_2 is long compared to $1/\gamma\Delta H$ (as it generally will be in a liquid), then the FID will be governed by $1/\gamma\Delta H$. We therefore cannot measure T_2 directly by looking at the FID signal, but must resort to the clever spin-echo technique, originally devised by Hahn,[14] which will be discussed shortly.

3. Relaxation summary

In summary, it has been seen that fluctuating internal fields having frequency components at the Larmor frequency can cause both T_1 and T_2 relaxation. T_2 relaxation can be produced by all three spatial components of the fluctuating field (x,y,z), whereas T_1 relaxation can only be caused by the transverse (x,y) components. This is due to the fact that the only nonzero matrix elements between energy states are due to the operators μ_x and μ_y. In addition, T_2 relaxation can be produced by a static component of the internal field [i.e., the zero frequency component of $J(\omega)$].

In a pure liquid or gas where molecular motion is random and rapid, $T_1 = T_2$. In a solid or viscous liquid where the internal field can have a large static component, $T_2 \ll T_1$. A liquid might have $T_1 = T_2$ above the freezing point, and when the liquid freezes, we get a sudden drop in T_2 such that $T_2 \ll T_1$. In an NMR experiment on tissue, our signal is obtained from protons on unbound water molecules or protons in fat; however, due to exchange between water bound to macromolecules and free water, $T_2 < T_1$. In pure water, $T_1 \approx T_2 \approx 3$ s, however, in brain tissue, at a resonant frequency of 2.7 MHz (corresponding to a field of 634 G), $T_1 = 285$ ms and $T_2 = 75$ ms. At 15 MHz, the relaxation times for brain tissue are $T_1 = 488$ ms, $T_2 = 78$ ms. Tissues which have a high water content (e.g., tumor or edematous tissue) have a greater proportion of unbound water and hence a longer T_1.

In addition, it has been noted that T_1 and T_2 are dependent on the Larmor frequency (hence the magnetic field strength) and the sample temperature. Note also that in practical experiment, the free-induction signal will decay in a time much shorter than T_2 due to inhomogeneities in the external field.

C. Measurement of T_1

A technique commonly used for T_1 measurements is inversion recovery. The pulse sequence is $180° - \tau - 90°$ as described below. If a 180° pulse is applied to sample (initially at equilibrium with a magnetization M_0 along the z axis), the magnetization will be rotated onto the $-z$ axis. The z component of the magnetization would then relax from $-M_0$, through 0, to $+M_0$. If the Bloch Eq. (26) is solved with the initial conditions $M_z(0) = -M_0$, we obtain

$$M_z(t) = M_0(1 - 2e^{-t/T_1}). \tag{31}$$

The transverse component would remain equal to zero and a FID signal would never be obtained. We can, however, sample M_z at any time by applying a 90° pulse at a time τ after the 180° pulse. This will rotate whatever component of M_z is present at time τ into the xy plane to give a FID signal. If, as usual, the rf signal $\mathbf{H}_1$ is applied along the x' axis, such that M nutates clockwise around the x' axis in the rotating frame on to the y' axis, the FID signal will be proportional to $M_{y'}$. If

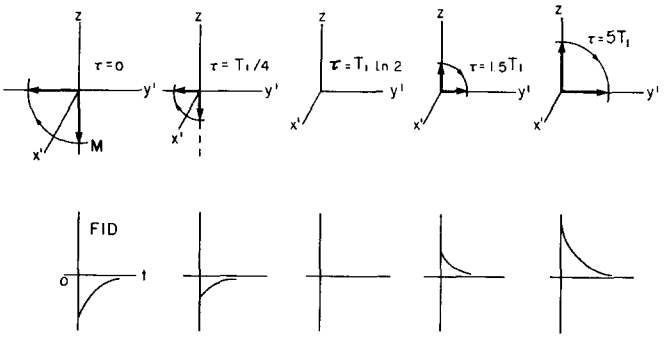

FIG. 9. Inversion-recovery sequence ($180° - \tau - 90°$) used for measuring T_1. The result of the 90° pulse is depicted for various time intervals τ.

the 90° pulse were applied immediately after the 180° pulse, then $M_{y'} = -M_0$ (**M** would lie along the $-y'$ axis). Figure 9 shows the effect of the 90° pulse in the rotating frame at various times τ. If the interval τ is varied until the signal passes through zero and then grows positive, T_1 could be found by noting the null point $\tau_{\text{null}} = T_1 \ln 2$. A better method would be to vary τ over a wide range, and fit the data with Eq. (31).

D. Measurement of T_2 (spin echoes)

As previously mentioned, true T_2 relaxation often is masked by external field inhomogeneities which cause a rapid decay of the FID signal. If we consider a sample which is divided into incremental segments, each one small enough to feel a uniform external field and each one having an incremental magnetization $\mathbf{m}_i$, then the individual $\mathbf{m}_i$ will dephase in the rotating frame as previously illustrated in Fig. 8, such that the net magnetization $\mathbf{M} = \Sigma \mathbf{m}_i$ disappears due to the external field inhomogeneity. For illustrative purposes, consider a three-region sample as shown in Fig. 10. If a 90° pulse is applied with $\mathbf{H}_1$ along the x' axis in the rotating frame in order to rotate all the $\mathbf{m}_i$ onto the y' axis [Fig. 11(a)], after termination of the pulse, $\mathbf{m}_0$ will remain at rest in the rotating system, $\mathbf{m}_+$ will precess faster than $\mathbf{m}_0$, and $\mathbf{m}_-$ slower than $\mathbf{m}_0$ in the lab, hence we get dephasing in the rotating system as shown in Fig. 11(b).

Suppose that a 180° pulse having $\mathbf{H}_1$ along the y' axis is then applied at a time τ after the 90° pulse. (Recall that the pulse can be shifted from the x' to the y' axis simply by phase shifting the rf signal by 90°.) This will cause the $\mathbf{m}_i$ vectors to precess clockwise about $\mathbf{H}_1$ in the rotating frame (i.e., about the y' axis). Since $\mathbf{m}_0$ already lies along the y' axis, it will not move, however, $\mathbf{m}_+$ and $\mathbf{m}_-$ exchange positions as shown in Fig. 11(c). This now puts the fastest moment $\mathbf{m}_+$ behind and the slowest $\mathbf{m}_-$ ahead, hence the spins will recluster at a time $t = 2\tau$ [Fig. 11(d)].

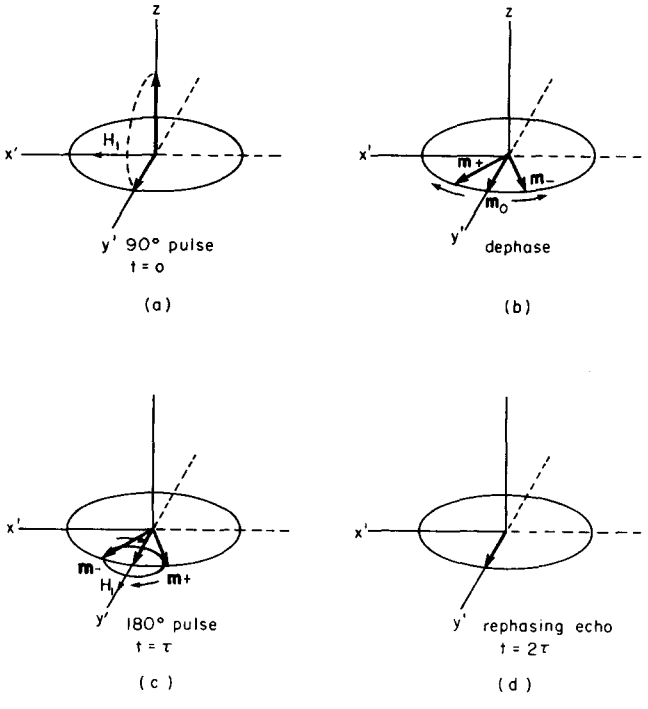

FIG. 11. CPMG spin-echo technique ($90°_{x'} - \tau - 180°_{y'}$).

The FID signal, which had decayed significantly by time τ due to the external magnetic field inhomogeneity, has now increased again, producing a "spin–echo" at time $t = 2\tau$. If time τ is long enough such that the FID signal has completely disappeared ($\tau \gg 1/\gamma \Delta H$), then an echo signal will be obtained as shown in Fig. 12. This signal has the shape of two FID signals back-to-back, since the spins must rephase in the same manner in which they initially dephased.

The height of the echo would be the same as the original FID signal at time $t = 0$ if it were not for *true* T_2 relaxation. That is, the moments $\mathbf{m}_+$, $\mathbf{m}_0$, and $\mathbf{m}_-$ are gradually decreas-

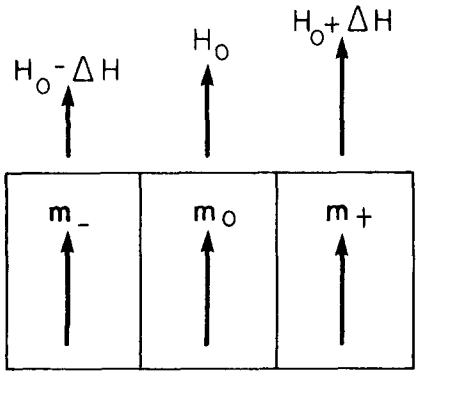

FIG. 10. A sample in a nonuniform external field, divided into segments small enough such that the magnetization in each incremental segment experiences a uniform, external magnetic field.

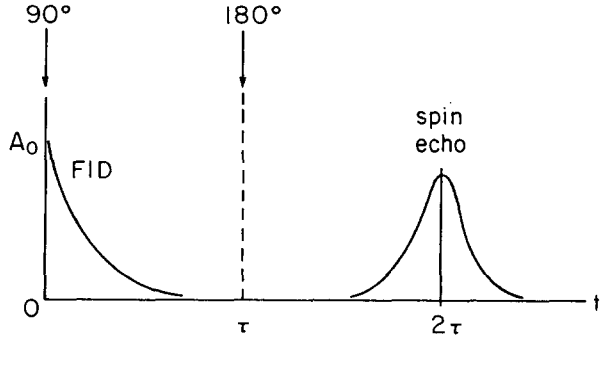

FIG. 12. Spin-echo signal produced by CPMG techique.

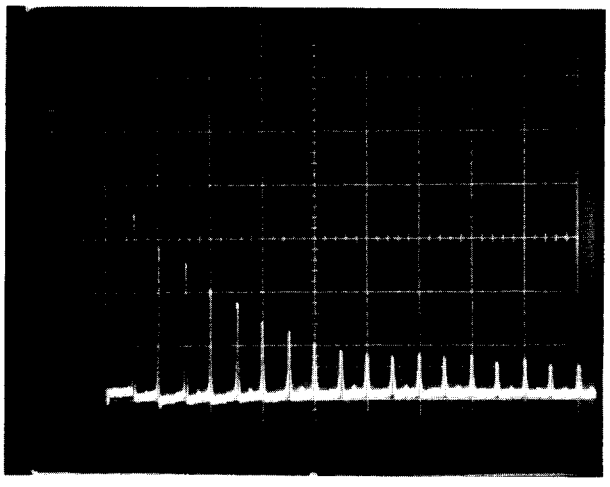

FIG. 13. CPMG repeated sequence. Multiple-spin echoes at $2\tau,4\tau,6\tau,...$ produced by repeating the 180° pulse at intervals of $\tau,3\tau,5\tau,...$. The echoes decrease in magnitude due to T_2 relaxation as $\exp(-2n\tau/T_2)$. The 180° pulses produce no signal, but they may be seen as blips on the baseline between the echoes.

ing in length due to internal field fluctuations (which cause the individual microscopic spins to dephase), but not to the external field inhomogeneity. The height of the echo at time 2τ is therefore given by

$$A(2\tau) = A_0 e^{-2\tau/T_2}, \tag{32}$$

where A_0 is the initial amplitude of the FID signal. If the sequence shown in Fig. 12 was continued by applying another 180° pulse at time 3τ, another echo would appear at time 4τ. If the sequence is continued indefinitely, a series of echoes would be obtained as illustrated in Fig. 13, the envelope of the echoes following

$$A(t) = A_0 e^{-t/T_2}, \tag{33}$$

where $t = 2n\tau$. T_2 can therefore be determined from the envelope.

This is called a Carr–Purcell, Meiboom–Gill (CPMG) pulse sequence[15] and is denoted by $90^\circ_{x'} - \tau - 180^\circ_{y'} - 2\tau - 180^\circ_{y'} - 2\tau - 180^\circ_{y'} \ldots$.

A similar sequence of echoes can also be generated using a Carr–Purcell (CP) pulse sequence in which all pulses have $\mathbf{H}_1$ along the x' axis in the rotating frame, rather than phase shifting the 180° pulses by $\pi/2$. It can be shown that the Carr–Purcell sequence also generates a similar series of echoes; however, the echoes will alternate in sign since the reclustering occurs alternately along the $-y'$ and $+y'$ axes due to the fact that $\mathbf{m}_0$ is also rotated by 180° in the CP sequence.

The CPMG sequence is preferred in most instances, due to the fact that it can compensate for the fact that the 180° pulse may not be precisely 180° due to experimental uncertainty and/or nonuniformity of $\mathbf{H}_1$ over the sample. If the pulse were slightly less than 180°, say $180° - \delta$, the vectors $\mathbf{m}_+$ and $\mathbf{m}_-$ would end up slightly above and below the xy plane, respectively, resulting in an echo of reduced amplitude. After the next $180° - \delta$ pulse, they end up back in the xy plane and the echo at $t = 4\tau$ would be a full strength echo. With CPMG, the even numbered echos are the proper strength, whereas, with the CP sequence the error is cumulative and the apparent echo decay is faster than T_2.

VI. NMR IMAGING

In 1971, Damadian[25] showed that NMR had the possibility of distinguishing normal and malignant tissue. In 1973, Lauterbur[26] showed how an NMR image could be created by using magnetic field gradients and reconstruction techniques. Images of human anatomy were soon being made, beginning in 1977.[27,28]

Although this paper is not intended to cover imaging techniques, but rather basic principles, we would be remiss if we did not provide a transition to imaging for the reader, and apply the spin manipulations previously illustrated.

We will suppose initially that someone has provided us with a "slice" of tissue to image, as depicted in Fig. 14. (It will be explained later how a slice of an intact body can be selected.) If a 90° rf pulse is applied to the entire slice, all the spins in the slice will start precessing freely in the xy plane.

If then (after termination of the rf pulse) a small, linear magnetic field gradient is applied to the slice along the y direction, superimposed on the large field $\mathbf{H}_0$ along the z axis, such that the z component of the external field varies as $H_z(y) = H_0 + gy$ as shown in Fig. 14, the protons will begin to precess at different frequencies depending on their location along the y axis. The precession frequency will vary with y across the slice as

$$\omega(y) = \omega_0 + \gamma g y, \tag{34}$$

where $\omega_0 = \gamma H_0$, such that those protons in the shaded strip parallel to the x axis shown in Fig. 14 will all have the same precession frequency; and there exists a linear one-to-one relationship between y and precession frequency.

The shape of the FID signal from the entire slice will be complex, since it will consist of a superposition of many frequencies; however, a Fourier analysis of the signal provides information on how much of each frequency is present and thence the number of protons in each incremental strip of the slice. The Fourier transform $F(\omega)$ gives the strength of the

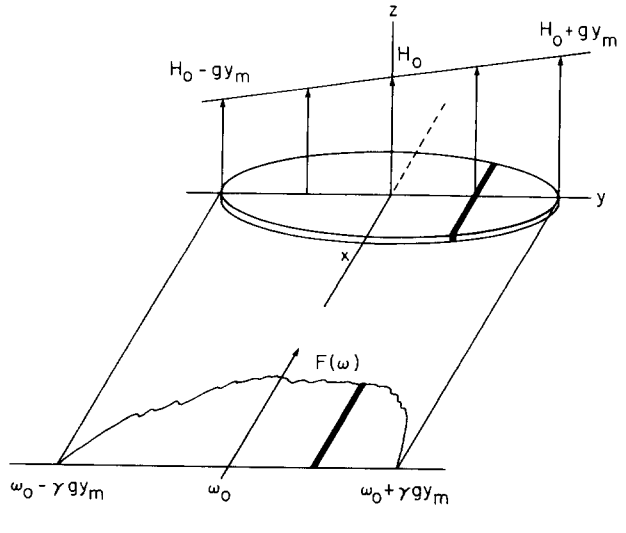

FIG. 14. Spin projection from a slice onto a line parallel to the magnetic field gradient.

signal from those protons precessing at frequency ω, and hence is proportional to the number of protons in the strip. Since there is a unique, linear relationship between ω and y, viz., $y = (\omega - \omega_0)/\gamma g$, $F(\omega)$ represents a spatial "projection" of proton density onto a line parallel to the gradient direction as depicted in Fig. 14, i.e., $F(\omega)$ can be written as $F(y)$.

By rotating the field gradient in, say, 1° increments over 180° and repeating this sequence at each angle (90° rf pulse, gradient application, and FID recording), 180 projections of the slice can be generated. CT reconstruction techniques (e.g., filtered back projection) can then be used to reconstruct from these projections the two-dimensional slice image on a display analogous to that of a CT image. That is, the slice is divided into pixels, and the proton density in each pixel is computed. The gradient can be rotated electrically[16] (a pair of gradient coils are located along the x and y axes), hence for NMR one does not need the mechanically rotating turret of x-ray CT.

A proton density image tends to have very little contrast, however, images enriched with T_1 or T_2 values can be generated in a similar fashion by using the appropriate pulse sequences. For example, the difference in proton density between grey and white brain matter is very small ($< 1\%$), however, the difference in T_1 at 2.5 MHz is about 23%.[17] The T_1 contrast ($\Delta T_1/T_1$) between muscle and various body tissues[18] is quite large (-25% to $+40\%$), hence T_1 images or T_1 enriched images will have the highest contrast.

A. Repeated FID sequence

Some T_1 dependence can be injected by repeating the above FID sequence (another 90° pulse) before the magnetization has a chance to reach its equilibrium value M_0 along the $+z$ axis.[19] If the time between 90° pulses is denoted by t_r, then M_z, which is initialized to zero after the 90° pulse, will have recovered to a value given by Eq. (27) at time t_r just before the next 90° pulse, and the value of the transverse component of M in the rotating frame after the repeated 90° pulse rotates M_z on to the y' axis is

$$M_{y'} = M_0(1 - e^{-t_r/T_1}). \tag{35}$$

This will be the value of a pixel in the image. If $t_r < T_1$, a T_1 dependence in the image is obtained, however, the FID signal strength is reduced. M_0 represents proton density.

B. Inversion recovery

A method to make the image strongly dependent on T_1 is to use the T_1 measurement technique of inversion recovery (Sec. V C); i.e., to apply a 180° pulse to the slice to invert M, apply a 90° pulse at a time τ later in order to sample $M_z(\tau)$, apply the readout xy gradient g_{xy} after termination of the 90° pulse to spatially encode the data and record the FID, and repeat the whole sequence at a time t_r after the 90° pulse. (That is, 180° — τ — 90° — t_r — 180°...with tranverse gradient g_{xy} application and readout occurring during the interval t_r.) Figure 15 shows schematically the spin manipulations that occur in the rotating frame. If $t_r \gg T_1$ such that the equilibrium magnetization recovers completely before the next 180° pulse, then the value of a pixel will be given by the same as the previously derived Eq. (31), viz.,

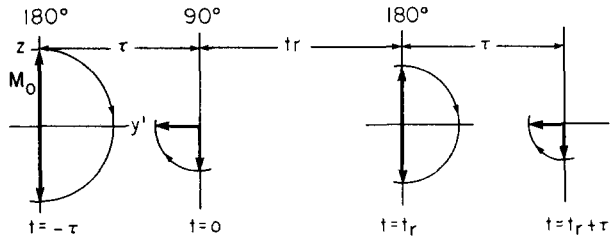

FIG. 15. Repeated inversion-recovery sequence.

$$M_{y'} = M_0(1 - 2e^{-\tau/T_1}). \tag{36}$$

Generally this is not a good assumption, since if one has to wait a long time ($\sim 5T_1$) between projection data collection, scan times will be quite long. If we assume that $t_r \gg T_2$ (since $T_2 \ll T_1$ for tissue) so that (as depicted in Fig. 15) no transverse component of spin remains before application of the next 180° pulse, then the analysis can be simplified. (We do not have to worry about spurious echoes.)

After the 90° pulse, M_z is initialized to zero, hence by the time t_r^- just prior to the next 180° pulse it will have recovered to the value given by Eq. (27).

$$M_z(t_r^-) = M_0(1 - e^{-t_r/T_1}). \tag{37}$$

The value of M_z immediately after the 180° pulse is the negative of the above, viz.,

$$M_z(t_r^+) = -M_0(1 - e^{-t_r/T_1}). \tag{38}$$

If the Bloch Eq. (26) is integrated between the limits t_r^+ and $(t_r^+ + \tau)$ with the initial condition Eq. (38), we obtain

$$M_z(t_r + \tau) = M_0[1 - 2e^{-\tau/T_1} + e^{-(t_r + \tau)/T_1}]. \tag{39}$$

Thus the value of $M_{y'}$ after the 90° pulse (the pixel value) is given by

$$M_{y'} = M_0[1 - 2e^{-\tau/T_1} + e^{-(t_r + \tau)/T_1}]. \tag{40}$$

Typical values of τ and t_r chosen for imaging at 6.25 MHz[19] are 400 ms and 1000 ms, respectively. In a volume element of the slice having a long T_1 (tumor or edematous tissue), where $\tau \ll T_1$, the value of $M_{y'}$ is negative since the inverted M is sampled while it is still along the $-z$ axis. For volume elements with a short T_1 (e.g., fat), where $\tau \gg T_1$, $M_{y'}$ is positive since the magnetization has recovered onto the positive z axis prior to the 90° sampling pulse.

C. Spin–echo sequence

It is also possible to generate images having T_2 dependence using spin echoes. If a pulse sequence 90° — τ — 180° — τ — t_r — 90°...is used, an echo appears at time τ after the 180° pulse (Sec. V D). The echo can be space encoded by applying the transverse readout gradient during its appearance, and it can be shown[19] that the pixel value will be given by

$$M_{y'} = -M_0 e^{-2\tau/T_2}[1 - 2e^{-(\tau + t_r)/T_1} + e^{-(2\tau + t_r)/T_1}], \tag{41}$$

such that the image depends on T_2. The factor outside the bracket will be recognized as the echo decay [Eq. (32)]. The term in the brackets is due to the fact that if t_r is not much

greater than T_1, the magnetization will not reach its full equilibrium value M_0 before the sequence is repeated. It is assumed in the foregoing that all pulses are applied with $\mathbf{H}_1$ along the x' axis.

D. Slice selection

A slice in an intact body may be selected for imaging by applying a field gradient in the z direction. In this case, the resonant frequency will vary along the axis of the body, hence each transverse plane will have a different resonant frequency $\omega(z)$. By varying the frequency of the rf pulses, the spins in any given transverse plane may be excited. If a z gradient g_z is applied during the 90° pulse in any of the aforementioned sequences, the spins only in a single narrow plane will be excited—the location of the plane depending on the excitation frequency selected. Of course, the slice is not as well defined as we like (it is more like a slice in conventional tomography), since those protons in the top and bottom of the slice will be slightly off resonance and will not end up exactly on the y' axis in the rotating frame after the $\pi/2$ pulse. It turns out[19] that if the z gradient is reversed for a short time after termination of the 90° rf pulse, spins will be rephased such that we have more nearly a pure 90° pulse throughout the slice, and much better slice definition.

There are many other methods of volume selection used in NMR (e.g., point, line, or plane); or, the signal from an entire three-dimensional object can be recorded as previously described. However, discussion of these methods is beyond the scope of this paper.[5]

[1]A. Abragam, *The Principles of Nuclear Magnetism* (Oxford University, London and New York, 1961).
[2]T. C. Farrar and E. D. Becker, *Pulse and Fourier Transform NMR* (Academic, New York, 1971).
[3]E. Fukushima and S. B. W. Roeder, *Experimental Pulse NMR—A Nuts and Bolts Approach* (Addison-Wesley, Reading, Massachusetts, 1981).
[4]C. P. Slichter, *Principles of Magnetic Resonance* (Harper and Row, New York, 1963).
[5]L. Kaufman, L. E. Crooks, and A. R. Margulis, *Nuclear Magnetic Resonance Imaging in Medicine* (Igaku-Shoin, New York and Tokyo, 1981).
[6]*NMR Imaging, Proceedings of an International Symposium on Nuclear Magnetic Resonance Imaging*, edited by R. L. Witcofski, N. Karstaedt, and C. L. Partain (Bowman Gray School of Medicine, Winston-Salem, North Carolina, 1982).
[7]A. Messiah, *Quantum Mechanics* (North-Holland, Amsterdam, 1961), Vol. I, p. 210.
[8]C. P. Slichter, *Principles of Magnetic Resonance* (Harper and Row, New York, 1963), p. 14.
[9]Reference 8, p. 17.
[10]H. Goldstein, *Classical Mechanics* (Addison-Wesley, Reading, Massachusetts, 1950), p. 133.
[11]J. D. Jackson, *Classical Electrodynamics* (Wiley, New York, 1962), p. 153.
[12]N. Bloembergen, *Nuclear Magnetic Relaxation* (Benjamin, New York, 1961).
[13]J. D. Jackson, *Classical Electrodynamics* (Wiley, New York, 1962), p. 143.
[14]E. L. Hahn, Phys. Rev. **80**, 580 (1950).
[15]S. Meiboom and D. Gill, Rev. Sci. Instrum. **2**, 688 (1958).
[16]P. A. Bottomley, in *NMR Imaging, Proceedings of an International Symposium on Nuclear Magnetic Resonance Imaging*, edited by R. L. Witcofski, N. Karstaedt, and C. L. Partain (Bowman Gray School of Medicine, Winston-Salem, North Carolina, 1982), pp. 25–31.
[17]C. R. Ling, M. A. Foster, and J. M. S. Hutchinson, Phys. Med. Biol. **25**, 748 (1980).
[18]B. A. Coles, J. Natl. Cancer Inst. **57**, 389 (1976).
[19]I. R. Young, D. R. Bailes, M. Burl, A. G. Collins, D. T. Smith, M. J. McDonnell, J. S. Orr, L. M. Banks, G. M. Bydder, R. H. Greenspan, and R. E. Steiner, J. Comput. Tomography **6**, 1 (1982).
[20]D. I. Hoult, in *NMR Imaging, Proceedings of an International Symposium of Nuclear Magnetic Resonance*, edited by R. L. Witcofski (Bowman Gray School of Medicine, Winston-Salem, North Carolina, 1982), pp. 33–39.
[21]C. P. Slichter, *Principles of Magnetic Resonance* (Harper and Row, New York, 1963), p. 28.
[22]D. I. Hoult and R. E. Richards, J. Magn. Reson. **36**, 447 (1979).
[23]B. L. Cohen, *Concepts of Nuclear Physics* (McGraw-Hill, New York, 1971), p. 174.
[24]D. M. Kramer, in *Nuclear Magnetic Resonance Imaging in Medicine*, edited by L. Kaufman, L. E. Crooks, and A. R. Margulis (Igaku-Shoin, New York and Tokyo, 1981), p. 184.
[25]R. Damadian, Science **177**, 1151 (1971).
[26]P. C. Lauterbur, Nature (London) **242**, 190 (1973).
[27]P. Mansfield and A. A. Maudsley, Br. J. Radiol. **60**, 188 (1977).
[28]R. Damadian, M. Goldsmith, and L. Minkoff, Physiol. Chem. Phys. **9**, 97 (1977).